

## Determination of Electron and Positron Helicity with Møller and Bhabha Scattering\*†

J. D. ULLMAN,‡ H. FRAUENFELDER, H. J. LIPKIN,§ AND A. ROSSI||  
*University of Illinois, Urbana, Illinois*

(Received November 16, 1960)

The determination of the helicity of electrons and positrons from beta decay by means of electron-electron (Møller) and positron-electron (Bhabha) scattering is discussed. The theoretical background, the apparatus, and the experimental procedure are treated in detail. The apparatus included, in addition to the conventional parts, a beta monochromator with a momentum resolution of 16% for the investigation of the energy dependence of the helicity. Experiments were performed with  $P^{32}$ ,  $Au^{198}$ , RaE, and  $Ga^{68}$ . In all cases, the helicities  $P$  were found to be proportional to  $v/c$ . The measured helicities, in units of  $v/c$  and averaged over the observed range of energies, are summarized as follows. (The errors given are statistical only; systematic errors are estimated to be less than  $\pm 3\%$ ).

Radioisotope	$P^{32}$	$Au^{198}$	RaE	$Ga^{68}$
Particles	$e^-$	$e^-$	$e^-$	$e^+$
Energy interval in keV	660-990	460-810	520-950	1030, 1300
Helicity $P/(v/c)$	$-1.00 \pm 0.02$	$-0.98 \pm 0.03$	$-0.75 \pm 0.03$	$+0.99 \pm 0.09$

### 1. INTRODUCTION

BETA decay today is much better understood than it was before the discovery that weak interactions do not conserve parity. Although the question of the fundamental nature of weak interactions remains open,<sup>1</sup> it is possible to explain a large body of experimental data with a simple and elegant theory, based in part on the description of the neutrino by a two-component wave function.<sup>2-4</sup> Experimentally it is of interest to see to what extent such a description is correct. The determination of the helicity of electrons and positrons emitted in beta decay yields one approach to this problem. The two-component neutrino and the corresponding theory of beta decay predict complete parity nonconservation, and this in turn implies a helicity  $P = -v/c$  for electrons and  $+v/c$  for positrons emitted in allowed beta transitions. Careful measurements of the helicity therefore are valuable for building a firmer foundation for the fundamental theory of beta decay.

While helicity experiments on allowed transitions help to elucidate the laws of beta decay, investigations on forbidden transitions can give information about nuclear matrix elements, and, hopefully, also about time-reversal invariance and conserved vector current

effects. In certain forbidden beta decays, such as RaE, the usually dominant matrix elements interfere destructively. The resulting spectrum shape can differ from the shape typical for the order of forbiddenness, and the electron polarization can be smaller than  $v/c$ . An accurate knowledge of the energy dependence of the polarization, in combination with the spectrum shape, allows the relative magnitude of several matrix elements to be fixed. The values of these matrix elements are expected to show the effects of a possible violation of time-reversal invariance in beta decay. Moreover, the calculation of these matrix elements from a nuclear model is strongly influenced by the conserved vector current theory of beta decay. Unfortunately, the calculations involved are difficult, and it is at the present time not uniquely possible to separate nuclear model assumptions, time-reversal invariance, and conserved vector current effects.

The first measurements of electron helicities were reported soon after the discovery of parity nonconservation. They employed the Mott scattering technique and were of an exploratory character. Since then this method has been refined and new approaches have been developed. For descriptions of the early experiments, discussions of the various methods, and for more complete lists of publications, we refer to other papers.<sup>5-7</sup> Among the various possibilities, the Mott scattering and Møller scattering methods appear capable of the highest accuracy. The Mott scattering method is based on the spin-orbit interaction in Coulomb scattering from heavy nuclei; it is at its best at non-relativistic energies and it is not easily applicable to positrons. The Møller scattering method depends on the spin dependence of electron-electron and positron-electron scattering; it works best at relativistic energies

\* Supported in part by the joint program of the Office of Naval Research and the U. S. Atomic Energy Commission.

† This paper is based on a thesis submitted in partial fulfillment of the requirements for the degree of Doctor of Philosophy at the University of Illinois. (J.D.U.)

‡ Present address: Institut de Recherches Nucléaires, Université de Strasbourg, Strasbourg, France.

§ Present address: Weizmann Institute of Science, Rehovoth, Israel.

|| Present address: Centro Ricerche Nucleari, Sorin, Saluggia, Vercelli, Italy.

<sup>1</sup> T. D. Lee and C. N. Yang, *Phys. Rev.* **119**, 1410 (1960).

<sup>2</sup> E. J. Konopinski, *Ann. Rev. Nuclear Sci.* **9**, 99 (1959).

<sup>3</sup> M. Gell-Mann, *Revs. Modern Phys.* **31**, 834 (1959).

<sup>4</sup> R. P. Feynman and M. Gell-Mann, *Phys. Rev.* **109**, 193 (1958).

<sup>5</sup> L. Grodzins, *Progr. Nuclear Phys.* **7**, 163 (1959).

<sup>6</sup> L. A. Page, *Revs. Modern Phys.* **31**, 759 (1959).

<sup>7</sup> H. Frauenfelder, *Nuovo cimento* (to be published).

and it can easily be used with positrons. These two methods complement each other in a fortunate way.

In the present paper, we report in detail on the Møller and Bhabha scattering method. The beauty of this technique lies in its extreme simplicity. In the first experiment reported,<sup>8</sup> the equipment consisted only of a source, a collimator, a magnetized deltamax scattering foil, two electron detectors, and a coincidence circuit. Such a setup worked well for electrons from beta decays not plagued by abundant gamma rays. It led, however, to erroneous results when it was applied to complicated decays.<sup>9</sup> Further improvements of the method included crude energy selection of the incident beta particles,<sup>10,11</sup> and thus overcame some of the difficulties apparent in the earlier work. In the investigation reported here, a further step was taken by adding a magnetic-lens beta monochromator to eliminate undesirable gamma-ray background and to select monoenergetic electrons. Furthermore, the corrections required to calculate the helicity values from the experimental data were studied carefully.

Four radioisotopes were investigated.  $P^{32}$ , an allowed Gamow-Teller transition, shows the expected helicity of  $-v/c$  to within 2%.  $Au^{198}$ , a first forbidden transition with allowed spectrum shape, also produces complete polarization,  $-v/c$ , to within 3%.  $Ga^{68}$ , an allowed Gamow-Teller positron emitter, yields full polarization,  $+v/c$ , with the  $+$  sign as expected for positrons. The statistical error in this experiment is  $\pm 9\%$ . RaE, the well-known first-forbidden transition with anomalous spectrum shape, had already been shown to possess a polarization considerably lower than  $v/c$ .<sup>11,12-14</sup> The present result,  $P = -(0.75 \pm 0.03)v/c$ , confirms the earlier data and extends them to higher energies.

After this introduction, the material in this paper is organized into five sections: 2. The Møller scattering method; 3. Apparatus; 4. Experimental procedure; 5. Results; and 6. Discussion.

## 2. THE MØLLER SCATTERING METHOD

### 2.1 Basic Aspects

#### 2.11 Polarization Dependence of the Cross Section

Electron-electron scattering can be used to measure electron polarization because the cross section for it is strongly polarization dependent. If the two colliding electrons have parallel polarizations, the cross section is smaller than if they have antiparallel polarizations.

<sup>8</sup> H. Frauenfelder, A. O. Hanson, N. Levine, A. Rossi, and G. DePasquali, *Phys. Rev.* **107**, 643 (1957).

<sup>9</sup> H. Frauenfelder, A. O. Hanson, N. Levine, A. Rossi, and G. DePasquali, *Phys. Rev.* **107**, 910 (1957).

<sup>10</sup> N. Benczer-Koller, A. Schwarzschild, J. B. Vise, and C. S. Wu, *Phys. Rev.* **109**, 85 (1958).

<sup>11</sup> J. S. Geiger, G. T. Ewan, R. L. Graham, and R. D. MacKenzie, *Phys. Rev.* **112**, 1684 (1958).

<sup>12</sup> W. Bühring and J. Heintze, *Z. Physik* **153**, 237 (1958).

<sup>13</sup> A. I. Alikhanov, G. P. Eliseyev, and A. Liubimov, *Nuclear Phys.* **13**, 541 (1959).

<sup>14</sup> H. Wegener, *Z. Physik* **154**, 553 (1959).

This fact can be predicted by a naive application of the Pauli principle: If the electrons are in the same spin state, they cannot be in the same space state and hence cannot collide. The dependence on polarization is strongest for "head-on collisions", i.e., scattering by  $90^\circ$  in the c.m. system. For such collisions, the parallel polarization cross section vanishes entirely at non-relativistic energies and the polarization dependence remains strong at all energies. It weakens as the scattering angle departs from  $90^\circ$  and vanishes at  $0^\circ$  and  $180^\circ$ . Positron-electron collisions have the same polarization dependence as electron-electron collisions in the extreme relativistic limit, but the polarization dependence vanishes nonrelativistically. A more complete discussion of this subject is given by Page.<sup>6</sup>

Bincer<sup>15</sup> has calculated the polarization dependence of electron-electron, electron-positron, and electron-muon collisions for longitudinally polarized particles. His results are expressed in terms of  $\sigma_p/\sigma_a$ , where  $\sigma_p$  is the scattering cross section with polarizations parallel and  $\sigma_a$  is the scattering cross section with polarizations antiparallel. Raczka and Raczka<sup>16</sup> give expressions for the cross section with arbitrary initial polarizations and initial and final momenta. Both of these calculations are in lowest order, with no radiative corrections. Radiative corrections have recently been considered, but they do not influence the present experiment.<sup>17</sup>

#### 2.12 Relation between Polarization and Counting Rates

To use the polarization dependence of the Møller cross section in measuring electron polarization, electrons must be scattered by target electrons of known polarization, and some aspect of the scattering process must be measured. The troubles inherent in absolute measurements of cross sections can be avoided by measuring a quantity that depends on the ratio of cross sections for two polarization states of the target electrons.

One such quantity can be developed as follows. Let  $\mathbf{P}_1$  be the polarization vector of the electrons to be measured, while  $\mathbf{P}_2$  is the polarization vector of the target electrons. Let  $\sigma_+$  be the scattering cross section with both electrons completely polarized in the directions of  $\mathbf{P}_1$  and  $\mathbf{P}_2$ , while  $\sigma_-$  is the cross section with complete polarization but with the direction of  $\mathbf{P}_2$  reversed. The cross section for scattering of electrons with uncorrelated polarization will be  $(\sigma_+ + \sigma_-)/2$ . In the usual definition of polarization, the magnitude of  $\mathbf{P}$  is the fraction of particles that are fully polarized. Therefore, a fraction  $P_1 P_2$  of the collisions takes place between particles that are fully polarized, and have cross section  $\sigma_+$  or  $\sigma_-$ , depending on the direction of  $\mathbf{P}_2$ . The rest of the collisions have cross section  $(\sigma_+ + \sigma_-)/2$ .

<sup>15</sup> A. M. Bincer, *Phys. Rev.* **107**, 1434 (1957).

<sup>16</sup> R. Raczka and A. Raczka, *Bull. acad. polon. sci.* **6**, 463 (1958).

<sup>17</sup> G. Furlan and G. Peressutti, *Nuovo cimento* **15**, 817 (1960).

With  $\mathbf{P}_2$  in its original direction, the counting rate will be proportional to

$$C_+ = P_1 P_2 \sigma_+ + (1 - P_1 P_2)(\sigma_+ + \sigma_-)/2. \quad (1)$$

With the direction of  $\mathbf{P}_2$  reversed, it will be proportional to

$$C_- = P_1 P_2 \sigma_- + (1 - P_1 P_2)(\sigma_+ + \sigma_-)/2. \quad (2)$$

From these equations, one obtains

$$\frac{C_+ - C_-}{C_+ + C_-} = P_1 P_2 \frac{\sigma_+ - \sigma_-}{\sigma_+ + \sigma_-}. \quad (3)$$

The polarization dependence of the cross section is often expressed in terms of  $\sigma_-/\sigma_+$ , and experimental results are given in terms of  $\delta$ , the relative change in counting rate on polarization reversal:

$$\delta \equiv 2 \frac{C_+ - C_-}{C_+ + C_-} = 2 P_1 P_2 \frac{1 - \sigma_-/\sigma_+}{1 + \sigma_-/\sigma_+}. \quad (4)$$

### 2.13 Obtaining Polarized Target Electrons

To use the relations given above, one must have target electrons of known polarization whose direction of polarization can be reversed. Such electrons exist in a magnetized ferromagnetic foil. About 2 of 26 orbital electrons in iron are aligned at saturation. The fraction of electrons aligned can be obtained by measuring the magnetization of the foil. It is related to the magnetization through

$$f = M_s / N\mu, \quad (5)$$

where  $M_s$  is the magnetic moment per unit volume in the material due to electron spin,  $N$  is the number of electrons per unit volume, and  $\mu$  is the Bohr magneton.  $M_s$  is not equal to the total magnetic moment per unit volume in the material; in addition to  $M_s$  there is a small but significant orbital contribution.<sup>18</sup> The relative magnitudes of the spin and orbital contributions can be obtained from a measurement of the gyromagnetic ratio for the foil material by an Einstein-de Haas or Barnett experiment.  $M_s$  is related to the total magnetization  $M$  by

$$M_s = 2 \frac{g' - 1}{g'} M, \quad (6)$$

where  $g'$  is the gyromagnetic ratio. For most magnetic materials,  $M_s$  is smaller than  $M$  by about 5%.

Measurements of  $g'^{19,20}$  are plentiful for pure elements, but rarer for the alloys likely to be used as scattering foils in a Møller scattering experiment. However, the results of Barnett and Kenney<sup>21</sup> permit reasonable estimates of  $g'$  for most ferromagnetic

alloys. These authors find that  $g'$  varies approximately linearly as a function of composition for binary Fe-Co-Ni alloys.

### 2.14 Detecting Møller Collisions

The cross section for Møller scattering from all electrons of an atom is smaller than the Mott cross section for scattering from the nucleus by a factor of about the atomic number of the scatterer. Therefore, Møller scattered electrons must be detected among a much larger number of Mott scattered ones. Fortunately, there are differences between Mott scattered and Møller scattered electrons. The Møller scattered ones come from collisions between particles of equal mass. In such collisions, as seen in the lab system, the incident electron gives up much of its kinetic energy to the target electron, and both emerge from the collision. This allows Møller collisions to be distinguished from the Mott background by counting the two electrons in coincidence.

Use of coincidence counting is helped by the fact that Møller scattering can be treated as a two-body process as long as the bombarding energy is much greater than the binding energy of the target electrons. If the incident momentum is known, there is a fixed relation between the momenta of the two outgoing electrons. The counters can be placed so that if one electron reaches one counter, the other electron will almost certainly reach the other. This relation can be obscured by multiple scattering in the foil, a problem that will be considered in 2.7.

Energy conservation in the collision can be used to discriminate against spurious coincidences by requiring the energies of the two electrons to add up to the incident energy. In our experimental arrangement, where collisions with 90° c.m. scattering angle were being counted, each electron's energy was required to lie in a narrow range around half the incident energy.

### 2.15 Experimental arrangement

Figure 1 shows the experimental arrangement. A magnetized ferromagnetic foil provides polarized target electrons and coincidence counting is used to detect Møller collisions. The angle  $\theta$  is the laboratory scattering angle corresponding to a 90° c.m. scattering angle. A beta monochromator selects electrons in a momentum band of 16%. The Møller scattered electrons at

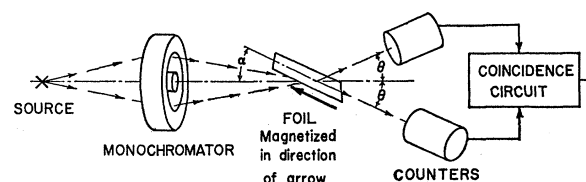


FIG. 1. Basic arrangement for the measurement of electron and positron helicity by means of Møller and Bhabha scattering.

<sup>18</sup> C. Kittel, *Introduction to Solid State Physics* (John Wiley & Sons, New York, 1956) 2nd edition, pp. 408-414.

<sup>19</sup> J. P. Meyer and S. Brown, *J. phys. radium* **18**, 161 (1957).

<sup>20</sup> G. G. Scott, *Phys. Rev.* **104**, 1497 (1956).

<sup>21</sup> S. J. Barnett and G. S. Kenney, *Phys. Rev.* **87**, 723 (1952).

90° c.m. scattering angle possess half the selected energy. Pulse-height analysis in the two counters thus distinguishes the Møller scattered electrons from those which have undergone Coulomb scattering. Energy selection and coincidence arrangement together form a very effective means for singling out the desired events.

For the measurement of longitudinal polarization, the target electrons should be polarized in the direction of the incident electron beam. Unfortunately, extremely high fields are necessary to magnetize a thin foil in a direction normal to its surface. Therefore, it is necessary to magnetize the foil along its surface and incline it at an angle to the electron beam, as shown in Fig. 1.

If the fraction of electrons aligned in the foil is  $f$ , and the angle of inclination of the foil to the electron beam is  $\alpha$ , the target electrons will have longitudinal polarization  $f \cos\alpha$  when looked at in the c.m. system. The transverse component of the polarization does not affect the scattering at 90° in the c.m. system, or in the plane normal to itself. The location of the counters as shown in Fig. 1 meets both these conditions. Thus, in Eq. (4) we can let  $P_2 = f \cos\alpha$  and  $\sigma_-/\sigma_+ = \sigma_p/\sigma_a$  for longitudinal polarization, as calculated by Bincer. Equation (4) then becomes

$$\delta = 2P_1 f \cos\alpha R, \quad (7)$$

$$R \equiv [1 - \sigma_p/\sigma_a] / [1 + \sigma_p/\sigma_a]. \quad (7')$$

## 2.2 Corrections

### 2.2.1 Effect of Finite Apertures and Energy Resolutions

The relations (7) are true for a single energy, scattering angle, and angle between the trajectory of electrons and the axis of the foil. In an actual experiment, a fairly wide range of all three of these quantities has to be accepted to get a reasonable counting rate. The problem of averaging the expression on the right of Eq. (7) over all the accepted events is, in general, very complicated.

The problem is simplified if the accepted energy range is reasonably narrow. Except at low energy, where the Møller scattering method is not at its best anyway, both  $\sigma_p/\sigma_a$  and  $P_1$  vary slowly with energy.  $P_1$  can then be treated as a constant, and  $\sigma_p/\sigma_a$  can be calculated at the mean accepted energy.

The averaging of  $\cos\alpha$  over electron trajectories can be separated from the averaging of  $R$  over scattering angles as long as the accepted distribution of scattering angles does not vary appreciably over the range of variation of  $\alpha$ . This can be assured by making the counter faces large enough.

The averaging of  $\cos\alpha$  over electron trajectories is a straightforward geometry problem. Averaging  $R$  over scattering angles is more complicated. First, one must know the distribution in scattering angle of the counted events. Controlling this distribution is helped by the fact that, in Møller scattering, there is a definite rela-

tion between the scattering angle and the energy of an electron after the collision. This correlation is important, because the energy will hardly be changed by multiple scattering that radically changes the direction of motion. It is possible to limit the accepted range of scattering angles by limiting the accepted range of energies. If the counters are large enough to intercept all the electrons allowed by the energy selection, multiple scattering will have little effect on the accepted distribution.

The distribution of accepted events as a function of electron energy after scattering can be measured by sweeping a narrow channel across the energy range accepted by one counter. This procedure gives the distribution of Møller scattered electrons reaching the counter. The resulting curve, when multiplied by the energy sensitivity curve of the counter as used in the polarization measurement, yields the accepted distribution of events. Once this distribution is known, the averaging process can be carried out by numerical integration. The averaging process is discussed in more detail in the Appendix, where simplified methods of carrying it out are derived.

### 2.2.2 Effect of Foil Thickness

Experimentally, it is found that as the thickness of the foil is increased, the counting rate rapidly rises to a maximum, and then gradually decreases. The maximum is reached with a very thin foil, the energy loss of an electron traversing it often being less than 1% of the incident energy. The reason for this behavior is the strong influence of multiple scattering in the foil on the probability of counting a coincidence. First, consider only multiple scattering after the Møller collision. The farther from the back of the foil a collision takes place, the more likely the angular relation between the directions of the two electrons leaving the collision is to be disturbed by multiple scattering. When the mean multiple-scattering angle becomes comparable with the counter aperture as seen from the foil, the probability of counting a coincidence will begin to drop towards the probability of counting two electrons leaving the foil at random angles. Thus, most of the counted collisions in a thick foil take place near the back of the foil.

Multiple scattering before Møller scattering has the effect of widening the angular distribution of electron velocities as the electrons move towards the back of the foil. This distribution will have some nonzero width to begin with, and these electrons suffer less multiple scattering than electrons from Møller collisions because of their higher energy. Eventually, however, the angular distribution of these electrons will be appreciably widened in the region at the back of the foil contributing most of the counted events. With further increase in foil thickness, this will cause more counts to be lost from the back of the foil than are gained from the front, and the coincidence counting rate will decrease.

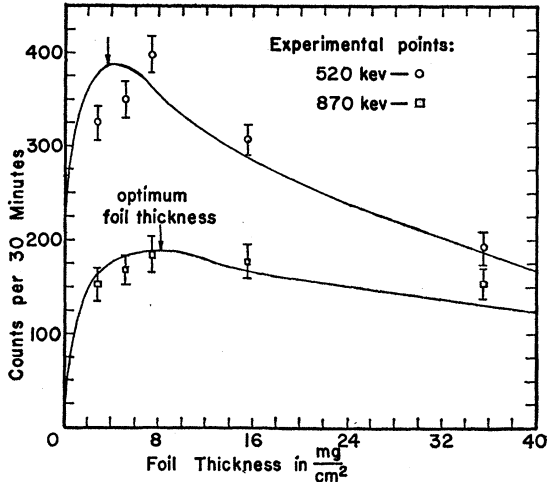


FIG. 2. Effect of scattering foil thickness on the coincidence counting rate. The solid lines correspond to the calculation outlined in section 2.22. The arrows show the foil thickness at which the root-mean-square scattering angle for the incident electrons equals the counter aperture.

To test the picture of multiple scattering in the foil, the coincidence rate as a function of foil thickness was calculated and compared with measurements. The calculation, in outline, went as follows: The counting rate at a depth  $x$  in the foil from a layer of thickness  $dx$  can be written

$$C(x) = F Y_1(x) Y_2(x) dx, \quad (8)$$

where  $F$  is the rate at which Møller collisions occur per unit foil thickness,  $Y_1$  is the probability that one electron from a Møller collision in  $dx$  will be counted,  $Y_2$  is the probability that the second electron from a Møller collision will be counted if the first is. Since the fraction of electrons scattered out of the beam is small in foils of the thickness used,  $F$  was treated as a constant.

$Y_1$  was found approximately by assuming the distribution of Møller scattered electrons from the foil (as a function of the angle of their trajectories to the axis of the instrument) to be a Gaussian, centered on the energy-equipartition angles. Its width is determined by the width of the beam striking the foil, the angular width corresponding to the accepted energy width, multiple scattering before the collision, and multiple scattering of the slower electrons leaving the collision. All these were assumed to be Gaussians, and their widths were added quadratically. Widths of the multiple-scattering distributions were assumed to vary as the square root of the distance traversed in the material, the constant of proportionality being evaluated from the formulas of Williams.<sup>22</sup>  $Y_1(x)$  was evaluated by finding the integral of this distribution across one counter face.

<sup>22</sup> E. J. Williams, Proc. Roy. Soc. (London) **A169**, 531 (1939). Williams' formulas are expressed in a convenient form by L. A. Kulchitsky and G. D. Latyshev, Phys. Rev. **61**, 254 (1942).

The distribution of second electrons from collisions from which the first electrons have been counted can be approximated in a similar way. It turns out not to have circular symmetry about the center of the second counter, but was taken to be a Gaussian with circular symmetry and of width equal to the root-mean-square width of the real distribution.  $Y_2$  is the integral of this distribution over the second counter face.

The coincidence counting rate as a function of foil thickness is given by

$$C(t) = F \int_0^t Y_1(x) Y_2(x) dx. \quad (9)$$

This quantity is shown for two incident electron energies and compared with measured counting rates in Fig. 2. The agreement with experiment is good enough to show that at least the general behavior of the counting rate is explained by multiple scattering. The arrows show the foil thickness at which the root-mean-square multiple scattering angle for the incident electrons equals the counter aperture. This appears to be a good, simple estimate of foil thickness for maximum counting rate.

The normalization of these curves is arbitrary. If they showed counting rates for equal electron flux, both would peak at about the same value. In Eq. (8),  $F$ , the rate at which Møller collisions occur per unit foil thickness, is proportional to the Møller cross section. If the foil is thick enough to produce a maximum counting rate, the integral is roughly proportional to the thickness of the layer at the back of the foil that is effective in contributing counted collisions. This is a thickness corresponding to a given multiple scattering distribution, which varies inversely as the Mott scattering cross section. The maximum counting rate for a given electron flux thus varies as  $\sigma_{\text{Møller}}/\sigma_{\text{Mott}}$ , which is nearly independent of energy.

## 2.3 Spurious Effects

There are effects other than Møller scattering in the foil which can influence the relative change in counting rate when the foil magnetization is reversed. These must be eliminated or accounted for. Effects of this kind which have been considered for our experiment are listed below.

### 2.31 Spurious Coincidences

An important class of spurious effects consists of coincidences not caused by Møller scattering in the foil. These usually are not affected by reversal of the foil magnetization, but reduce the relative change in counting rate. Some sources of spurious coincidences are briefly discussed.

*Accidental coincidences.* Since the accidental coincidence rate can be measured (by inserting a delay in one channel) and subtracted from the total rate, it does not

become troublesome until it becomes so large that it significantly increases the statistical uncertainty in the result. With our apparatus, coincidence counting rates of up to a few hundred per minute could be used without this happening.

*Counter-to-counter scattering.* An electron, reaching one of the counters with the full incident energy after Mott scattering in the foil, can be scattered into the other counter, leaving about half its energy in each counter. Such an event produces a true coincidence. The probability that this will happen depends on the size and location of the counters, but it is generally large if there is no obstruction between the counters. In our apparatus, these events made up about 30% of the total counting rate before the path between the counters was blocked with a thin lead absorber. With this absorber in place, these events contributed less than 1%.

*Bremsstrahlung from the foil.* A bremsstrahlung photon and the electron that produced it can make a true coincidence, which will be indistinguishable from a Møller coincidence if the electron loses about half its energy in producing the photon. The number of such electron-photon pairs can be appreciable. A comparison of differential cross sections (per unit energy loss of the electron) at 1-Mev incident energy and 50% energy loss shows that the bremsstrahlung cross section amounts to 12% of the Møller cross section.<sup>23</sup> The probability that these events will be counted, however, is small. The production of bremsstrahlung is a three-body process, so the correlation between the directions of emission of the two particles that characterizes Møller scattering is lost. If in addition the counters are made insensitive to gamma radiation, the beta-gamma coincidence rate can be made negligible.

*Other radiations.* Depending on the decay scheme of the radioactive source, other gammas or betas may be emitted in coincidence with each other or with the beta being measured. The number of resulting coincidences can be very large if the foil is not thoroughly shielded from direct gamma radiation from the source.

*Møller scattering in places other than the foil* can be minimized by keeping the electron beam well defined in the region of the foil and designing foil holders and other hardware so that they are well clear of the beam and do not have unobstructed paths between them and the counters. The number of these coincidences can be obtained by measuring the coincidence rate with the foil removed.

*Annihilation radiation when measuring positrons* produces two kinds of spurious coincidences. A positron annihilating somewhere between the counters can produce a gamma-gamma coincidence. A positron can also be counted in one counter, annihilated there, and one of its annihilation gammas can trigger the other counter. These spurious coincidences are minimized by

making the counters less sensitive to gamma rays (thin crystals), allowing the beam to freely leave the region of the counters, and discriminating against annihilation radiation by pulse-height selection.

The number of remaining spurious coincidences due to positrons can be measured as follows. An absorber thick enough to stop the positrons, but not the annihilation radiation, is placed over one counter. The counting rate measured will be  $C_1 = n_0 + n_1 + n_2$ , where  $n_0$  is the counting rate due to annihilation outside the counters,  $n_1$  that due to annihilation in one counter, and  $n_2$  that due to annihilation in one absorber. With identical absorbers over both counters, the counting rate will be  $C_2 = n_0 + 2n_2$ . The total spurious coincidence counting rate with no absorbers over the counters is  $n_0 + 2n_1$ , which is equal to  $2C_1 - C_2$ .

### 2.32 Spurious Changes in Counting Rate

A second class of spurious effects occurs if the reversal of the magnetization of the foil causes a change in the coincidence counting rate for any other reason than the change in Møller scattering cross section. This kind of effect can be detected by measuring the polarization of unpolarized electrons (conversion electrons are useful for this) since it will cause the result to be different from zero. It is, however, not sufficient to replace the foil with a nonferromagnetic foil. The field of the foil itself can cause a measurable change in counting rate on magnetization reversal.

The following are some of the ways in which a spurious change in counting rate can be produced:

*Influence of the magnetic field on the counters.* If the characteristics of the counters change when the foil magnetization is reversed, there will be a spurious change in counting rate. Multiplier phototubes are particularly sensitive to magnetic fields. If scintillation counters are used, all such tubes must be thoroughly shielded and removed from the vicinity of the foil and its magnetizing apparatus by light pipes.

*Influence of the magnetic field on electron trajectories.* The reversal of the foil magnetization will shift the angular distribution of electrons from Møller collisions slightly. The effect of this shift is minimized by carefully aligning the apparatus so that it is as nearly symmetrical as possible. Then, reversal of the magnetic fields at the foil will transform the electron trajectories into their mirror images about a plane passing through the axis of the instrument, and the new relation of electron trajectories to counters will be the mirror image of the old one. This effect can also be decreased by selecting the counted events by energy instead of angle. Then, a change in angular distributions will have little effect on the counting rate even if the apparatus is out of symmetry.

## 2.4 Depolarization

Electrons can be depolarized by multiple and single scattering in the source, and by multiple scattering in

<sup>23</sup> H. W. Koch and J. W. Motz, *Revs. Modern Phys.* **31**, 920 (1959).

the foil and any material between the source and the foil. Depolarization in the source is treated by Bienlein *et al.*<sup>24</sup> Mühlischlegel and Koppe<sup>25</sup> have calculated the depolarization of electrons passing through a thin layer of material.

Depolarization in the scattering foil cannot be treated by calculating the loss of longitudinal polarization caused by multiple scattering. This fact can be seen most easily in the nonrelativistic approximation. When a nonrelativistic electron is scattered by a nucleus, the orientation of its polarization vector in space is unchanged. If it subsequently collides with another electron, the value of  $\mathbf{P}_1 \cdot \mathbf{P}_2$  in the collision is unaffected by the previous scattering. Nonrelativistically,  $\sigma_p/\sigma_a$  depends only on  $\mathbf{P}_1 \cdot \mathbf{P}_2$ , so the polarization measurement will not be affected, even though the scattering has reduced the longitudinal polarization.

It is also instructive to look at the extreme relativistic approximation. Suppose an extremely relativistic electron is scattered through an angle  $\theta$  by a nucleus. Its polarization will be rotated through the same angle as its momentum, and its longitudinal polarization will not be changed. However, if it subsequently collides with a target electron polarized in its original direction of motion, the longitudinal polarization of the target electron in the center of mass system will be reduced by a factor of  $\cos\theta$ . This will reduce the measured value of the polarization of the incident electron by the same factor.

To treat the scattering in the foil properly, it is necessary to examine what happens to the expression for  $\delta$  when electrons are scattered before Møller collisions. According to Mühlischlegel and Koppe, the effect of multiple scattering through an angle  $\theta$  on an originally longitudinally polarized electron is approximated reasonably well by a rotation of the polarization vector through an angle of

$$\phi = \frac{\gamma - 1}{\gamma} \theta, \quad (10)$$

where  $\gamma$  is the total energy of the electron in units of  $mc^2$ . The angle  $\phi$  is just the rotation which the polarization vector would undergo if the electron were deflected through an angle  $\theta$  in a cylindrical condenser. The cross section for a collision between two initially longitudinally polarized electrons, one of which has previously been scattered through angle  $\theta$  and had its polarization rotated through angle  $\phi$ , can be taken from the formulas of Raczka and Raczka.<sup>16</sup> Doing this for the two states of target electron polarization, one obtains  $R = (1 - \sigma_-/\sigma_+) / (1 + \sigma_-/\sigma_+)$ , where  $\sigma_+$  is the cross section with polarizations initially parallel and  $\sigma_-$  is the cross section with polarizations initially antiparallel. The observed  $\delta$ , as defined in Eq. (4), is proportional to  $R$ . The relative change in  $\delta$  due to the

<sup>24</sup> H. Bienlein, K. Guthner, H. von Issendorf, and H. Wegener, *Nuclear Instr.* 4, 87 (1959).

<sup>25</sup> B. Mühlischlegel and H. Koppe, *Z. Physik* 150, 474 (1958).

multiple scattering will therefore be equal to  $(R - R_0)/R_0$ , where  $R_0$  is the value of  $R$  with no scattering previous to the Møller scattering ( $\theta = \phi = 0$ ). The expression obtained is

$$\begin{aligned} (R - R_0)/R_0 = & (7\gamma^2 - 6\gamma + 3)^{-1} \\ & \times \{ (\gamma^2 - 10\gamma + 5)(1 - \cos\phi) + 2(\gamma - 1)^2 \\ & \times [4(1 - \cos\theta \cos\phi) - \sin\theta \sin\phi] \}. \end{aligned}$$

When  $\phi$  is expressed in terms of  $\theta$  using Eq. (10), and the above expression is expanded as a power series in  $\theta$ , the series has only even powers of  $\theta$ . Keeping only the first nonvanishing term, one gets

$$\frac{R - R_0}{R_0} \approx \frac{(\gamma - 1)^2 (7\gamma^2 + 6\gamma + 3)}{2\gamma^2 (7\gamma^2 - 6\gamma + 3)} \theta^2. \quad (11)$$

This expression goes to zero as  $\gamma \rightarrow 1$ , and goes to  $\theta^2/2$  as  $\gamma \rightarrow \infty$ , becoming the first term in the expansion of  $1 - \cos\theta$ .

Electrons scattered through angles greater than the counter half aperture as seen from the foil are not likely to produce counted coincidences. The average value of  $\theta^2$  for all the counted events will therefore be less than the square of the counter half aperture. Since the coefficient of  $\theta^2$  is always less than  $1/2$ , the maximum possible value for this loss of effect will be very small if reasonably small counters are used; for our apparatus, less than 2%.

The preceding discussion does not consider the inclination of the foil, which gives the polarization of the target electrons the required longitudinal component. This inclination will have no effect as long as the distribution in scattering angle of electrons producing counted coincidences is symmetrical. This distribution, however, will not be symmetrical. Electrons scattered towards the plane of the foil will pass through more material than electrons scattered away from the plane of the foil; they will have more Møller collisions and their spins will be brought more into line with the spins of the target electrons. The result will be an increase in the polarization dependence of the Møller scattering, and a decrease in the loss of effect through multiple scattering.

The asymmetry in the distribution of electrons producing counted events will not be as large as appears at first sight. It was shown in 2.2 that, if a foil is thick enough to give a maximum counting rate, the probability of producing a counted coincidence depends more on multiple scattering after the Møller collision than on the thickness of material traversed. However, this will not remove the asymmetry entirely, so Eq. (11) should only be used to calculate an order of magnitude or an upper limit.

### 3. APPARATUS

The experimental arrangement is shown in Fig. 3. The monochromator, used to get an approximately



monoenergetic beam from the beta decaying sources, was of the short lens type, with the coils surrounded by an Armco-iron structure having a narrow gap. This design was chosen to allow high-energy electrons to be focussed with moderate current, and to minimize the magnetic stray field at the scattering foil.

One disadvantage of this design is the large spherical aberration that results from the nonuniformity of the magnetic field. This was more troublesome than expected. To make a countable Møller event, an electron must strike the foil at such an angle that the pair of electrons from the collision can reach the counters. Only electrons whose trajectories are directed towards a small region behind the scattering foil can do this. Thus, the useful transmission of the instrument was effectively limited by a small axial stop behind the scattering foil. With severe spherical aberration, only a small proportion of the electrons entering the entrance window of the spectrometer will go through this stop—in our case, about one third, giving an effective transmission of less than 0.2%.

An annular exit baffle of variable aperture was used to give adjustable momentum resolution. For all the measurements reported here, it was set to pass a momentum width of 16%. The energy calibration of the monochromator was performed with the conversion lines of Cs<sup>137</sup> (624 keV) and Hg<sup>208</sup> (194 keV), and the 1.17-MeV and 1.33-MeV gamma lines of Co<sup>60</sup>, converted in a lead foil. The momentum focussed was a linear function of magnet current within 2% up to 1.3 MeV.

The source and the counters were mounted outside the vacuum, electrons entering and leaving the vacuum through Mylar windows. The source window was 1 mil (3.6 mg/cm<sup>2</sup>) thick and the counter window, being much larger, was 1.5 mils thick and supported by 0.01-in. steel wires, 1 in. apart. External mounting makes servicing the counters and replacing the sources easier and eliminates the trouble given by evaporation of sources in the vacuum. The energy loss in the win-

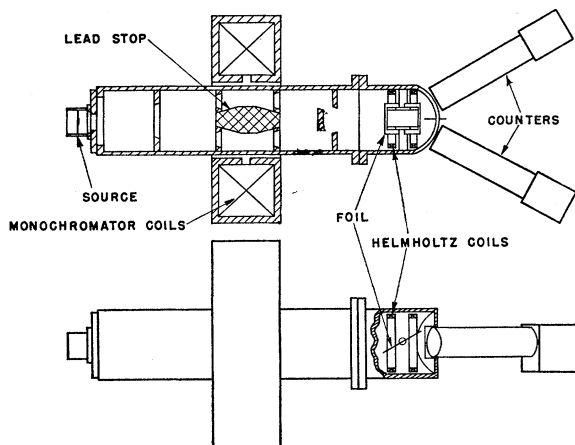


FIG. 3. Experimental realization of the arrangement shown schematically in Fig. 1.

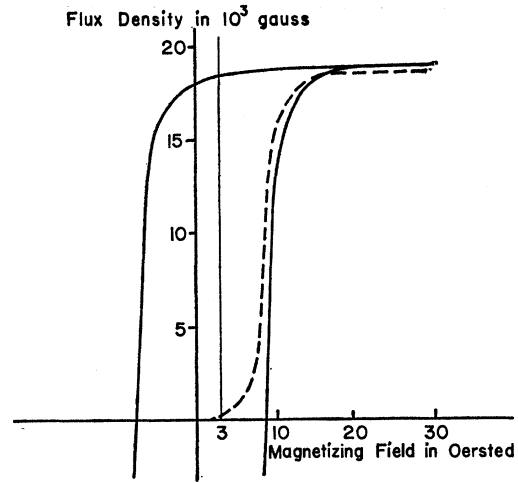


FIG. 4. Hysteresis and magnetization curves for a 0.2 mil Supermendur scattering foil.

dows and the short air paths just outside them was not troublesome at the higher energies used, but was beginning to be important at 500 keV and makes this system inadvisable at lower energies.

The scattering foils were of hydrogen-annealed Supermendur,<sup>26</sup> of 0.2 and 0.4 mils thickness. A hysteresis curve and a magnetization curve for a 0.2-mil foil are shown in Fig. 4. The magnetization curve shows the magnetization of the foil after being brought to a peak magnetizing field which was then reversed and brought back to a constant (3 oersted) holding field. The magnetization is independent of the peak magnetizing field (within the accuracy of the measurement) for peak magnetizing fields above about 20 oersteds. A magnetizing field of 30 oersteds was chosen for this foil. The magnetization of the foil was reversed between runs by discharging a large condenser through the magnetizing coils.

To calculate the fraction of electrons aligned in the foil, it is sufficient to know its composition, the atomic weights and atomic numbers of its constituents, its weight per unit length, and the total magnetic flux in the foil material when it is magnetized. Of these quantities, the most difficult to know is the magnetic flux. The method we used to measure it is standard and discussed in many textbooks, but the thinness of the foils causes difficulties in the measurement which merit some discussion here.

The flux in the foil was measured with the foil mounted in the apparatus and carried through its magnetization reversal exactly as between runs. The construction of the foil holder allowed a coil to be slipped over the foil. The change in flux through the coil was measured with a General Electric fluxmeter, and corrected for the magnetizing field and the leakage of flux from the foil back through the coil. The second of these

<sup>26</sup> H. L. B. Gould and D. H. Wenny, *Elec. Eng.* **76**, 208 (1957).



corrections (the correction for the "demagnetizing field") will be larger than in the case of thick samples and will have to be calculated. If it is assumed that the foil is uniformly magnetized to saturation, its field will be the known one of two finite line charges. This field must then be integrated over the extent of the coil to give the correction. Doing this to the necessary accuracy can be hard unless this correction is made as small as possible. One can minimize it by making the foil long and by keeping the cross section of the coil at a minimum. By winding the coil tightly on a thin copper form just fitting the foil holder, this correction was kept below 5% for the thinnest foil used.

To obtain a large and easily read fluxmeter deflection with a coil of small area, fine wire must be used. This leads to trouble because the drift rate of the fluxmeter is proportional to the resistance in its circuit. However, an appreciable drift can be accounted for by measuring the fluxmeter deflection with several values of added resistance in the circuit, plotting deflection as a function of resistance, and extrapolating to zero total resistance. For our foils, two sets of such measurements were made with different initial fluxmeter readings. This produced two such curves which had to extrapolate to the same deflection at zero resistance.

The fluxmeter calibration was checked at several values of deflection with a standard mutual inductance and a recently calibrated standard ammeter. This calibration was repeated at the end of the magnetic measurements. All measurements were repeated several times during the experiment to assure that the magnetic characteristics of the foils were not changing.

A pair of Helmholtz coils, their axes coinciding with the axis of the spectrometer, were used to magnetize the foil. This method was chosen instead of the iron yoke used earlier<sup>8</sup> because its field is mostly axial and reversing it should not affect electron trajectories seriously. This allows larger holding fields to be used.

Electrons from Møller collisions were counted by scintillation counters, located to receive electrons emerging from the foil at a 90° center-of-mass scattering angle. Electrons with the proper energy, arriving in time coincidence, were chosen by a fast-slow coincidence spectrometer.<sup>27</sup> Pulses from each counter were sent to a fast coincidence circuit with a resolving time of  $2\tau = 10^{-8}$  sec. Pulses were also sent to linear amplifiers followed by single-channel pulse-height analyzers. These selected pulses in the neighborhood of half the incident electron energy. Triple coincidences between pulses from the pulse-height analyzers and the fast coincidence circuits were counted as Møller events.

Plastic scintillators were used. During the measurements of electron polarization, these scintillators were 13 mm thick, this being the range of the most energetic

electrons that could be focussed by the monochromator. During the positron measurements, they were replaced by scintillators 5 mm thick to reduce the sensitivity to annihilation radiation. The scintillators were connected to RCA 6342 multiplier phototubes by straight 8-in. light pipes. Magnetic shielding of the phototubes included an inner mumetal shield and an outer shield of silicon iron.

#### 4. EXPERIMENTAL PROCEDURE

Data were taken with an automatic photographic recording system. A clock pulse, repeated at regular intervals, started a sequence of operations in which the scalers were stopped and photographed, the magnetization of the foil was carried through its reversal cycle, and the scalers were cleared and restarted.

The length of runs between reversals of foil magnetization was 20 minutes to 1 hour, depending on the counting rate. Tests were made to assure that, with the chosen run lengths, changes in counting rate due to drift in the electronics were small in comparison with the statistical variation in counting rate. Counting rates between 4 and 160 per minute were used. At the lowest rate, obtained with a Ga<sup>68</sup> source, data were taken for several weeks at each energy.

The accidental coincidence rate was measured and corrections made if necessary. At the highest counting rate, the accidental rate amounted to 5%. The coincidence rate with the foil removed was also measured and subtracted from the total coincidence rate. These spurious coincidences did not exceed 2% of the total rate. They vanished when an absorber just thick enough to stop the betas from Møller scattering was placed over either counter. It seems likely that they were caused by Møller scattering from stops in the monochromator.

The beta-gamma coincidence rate was measured by placing an absorber just thick enough to stop the betas over one counter. It was never more than a small fraction of a percent.

During the positron measurements, the counting rate due to annihilation radiation was determined by the method described in 2.3. At 1.03 Mev, annihilation produced 10% of the coincidences, and at 1.3 Mev, 5%.

During the 1.3-Mev run, the lead stop mounted between the counters to prevent counter-to-counter scattering was removed to reduce annihilation radiation. Counter-to-counter scattering was prevented by drawing the counters back into their shields. Later, measurements of the annihilation counting rate showed that, even with the lead stop in place, most of the counts came from annihilation in the scintillators. Therefore, during the 1.03-Mev run the stop was used and the counters moved forward to gain a better counting rate at the expense of a slight increase in annihilation background.

During a run, the pulse-height analyzers were set with channel centers at half the incident energy minus

<sup>27</sup> P. R. Bell and R. E. Bell in *Beta and Gamma Ray Spectroscopy*, edited by K. Siegbahn (North Holland Publishing Company, Amsterdam, 1955).

energy losses in reaching the counters. Channel width was usually set at about 50% of the channel center voltage. This choice resulted in a distribution of counted events with a width to half maximum of about 40%.

Since the energy width transmitted by the monochromator was fairly wide, the transmitted electron energy distribution depended on the shape of the beta spectrum as well as the monochromator current. For this reason, all the transmitted energy distributions were measured with a scintillation spectrometer calibrated with the  $\text{Cs}^{137}$   $K$ -conversion line. The values quoted for the midpoint energies of the electron distributions reaching the foil were taken from these measurements.

The energy calibration of the scintillation counters, linear amplifiers, and pulse-height analyzers was checked regularly by measuring the pulse-height spectra with the pulse-height analyzers while the apparatus was set up in the normal way during a run. The most prominent feature of these spectra was the peak at the incident energy due to Mott scattered electrons. The pulse-height analyzer base line and channel width settings were kept at fixed percentages of the voltage of this peak.

The  $\text{P}^{32}$  sources were obtained from Oak Ridge National Laboratory. All were of 25-mC strength. The phosphorus was in the form of  $\text{H}_3\text{PO}_4$  which was evaporated to dryness in a vacuum, usually on 4-mg/cm<sup>2</sup> aluminum backing. Average thickness of the active material was less than 1 mg/cm<sup>2</sup>.

The  $\text{Au}^{198}$  sources consisted of a layer of gold metal (1.3 or 2.2 mg/cm<sup>2</sup>) evaporated onto a 4-mg/cm<sup>2</sup> aluminum backing and neutron irradiated in the high flux region of the Argonne National Laboratories  $CP$ -5 reactor. An identical aluminum foil without gold was irradiated along with the gold plated one and checked for activity. It was about a factor of  $10^8$  weaker than the source at the time measurements were started. In addition, the half-life of the measured activity was checked by plotting the single and coincidence rates as a function of time.

The  $\text{RaE}$  source was 10 millicuries of radium ( $D+E$ ), furnished in a sealed source by the Canadian Radium and Uranium Corp. The active material was lead nitrate, of less than 0.2 mg/cm<sup>2</sup> averaged thickness, sandwiched between two layers of 1 mg/cm<sup>2</sup> aluminum.

The  $\text{Ga}^{68}$  source was  $\text{Ga}^{68}$  in equilibrium with its longer lived parent  $\text{Ge}^{68}$ . The active material was about 20 mg/cm<sup>2</sup> of germanium oxide between two layers of 1 mg/cm<sup>2</sup> Mylar. Source strength was about 2 millicuries. The  $\text{Ge}^{68}$  was produced by bombardment of  $\text{Ga}^{69}$  with protons in the Oak Ridge 86-in. cyclotron.

To test for spurious effects, conversion electrons from  $\text{Cs}^{137}$  were measured. The resulting asymmetry  $\delta = 1.010 \pm 0.058$  shows no spurious effects within the accuracy of the measurement.

TABLE I. Helicities of electrons and positrons from beta decay.

Radio-isotope	$\text{P}^{32}$	$\text{Au}^{198}$	$\text{RaE}$	$\text{Ga}^{68}$
Particles	$e^-$	$e^-$	$e^-$	$e^+$
Energy interval in kev	660-990	460-810	520-950	1030, 1300
Helicity $P/(v/c)$	$-1.00 \pm 0.02$	$-0.98 \pm 0.03$	$-0.75 \pm 0.03$	$+0.99 \pm 0.09$

## 5. RESULTS

The results are tabulated in Table I and shown in Fig. 5. The measured quantity is  $\delta = 2(C_p - C_a)/(C_p + C_a)$ , where  $C_p$  is the counting rate with the foil magnetized parallel to the incident electron beam, and  $C_a$  is the counting rate with it magnetized antiparallel to the beam. The polarization is related to  $\delta$  by

$$P = \frac{\delta}{2\langle \cos\alpha \rangle_{av} f R_{av}}, \quad (12)$$

where  $P$  is the polarization;  $\alpha$  is the angle between the momentum of the incident electron and the direction along which the foil is magnetized, and  $\langle \cos\alpha \rangle_{av}$  is the average of  $\cos\alpha$  over all accepted collisions;  $f$  is the fraction of electrons aligned in the foil; and  $R_{av}$  is  $R = (1 - \sigma_p/\sigma_a)/(1 + \sigma_p/\sigma_a)$  averaged over all accepted collisions. The value of  $\delta$  given is corrected for spurious coincidences (coincidences with the foil removed) and accidental coincidences.

The value of  $P$  given is corrected for depolarization in the source, the scattering foil, and all material between the source and the foil. For some sources (where the depolarization correction is marked with the letter "a") a correction for scattering from the source holder is included. These source holders allowed electrons to be scattered through  $90^\circ$  from them into the monochrom-

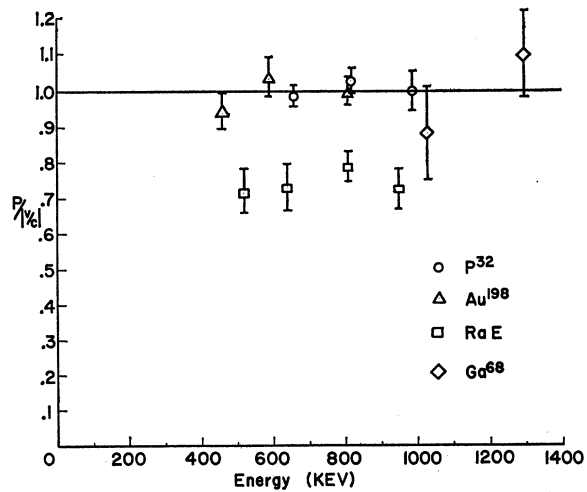


FIG. 5. Experimental results: polarization  $P$ , in units of  $v/c$ , versus kinetic energy of the electrons ( $\text{P}^{32}$ ,  $\text{Au}^{198}$ ,  $\text{RaE}$ ) or positrons ( $\text{Ga}^{68}$ ).

TABLE II. Experimental results. The table contains the measured values of the asymmetry [Eq. (4)], the average cross-section ratio  $R_{av}$  as defined in Sec. 2.21, corrections due to finite apertures and finite energy resolution (Sec. 2.21), corrections due to depolarization  $P$ .

Activity	Energy (kev)	Foil	$\delta$	$R_{av}$	$R(90^\circ) - R_{av}$		$P$	$P/(-v/c)$
					$R(90^\circ)$ (%)	Depolarization correction (%)		
$P^{32}, \beta^-$	660	1	$0.0840 \pm 0.0044$	0.816	6.6	3.8 <sup>a</sup>	$-0.891 \pm 0.047$	$0.983 \pm 0.029$
	660	1	$0.0850 \pm 0.0030$	0.816	6.6	1.5	$-0.882 \pm 0.031$	
	660 (sum)						$-0.885 \pm 0.026$	
	820	3	$0.0754 \pm 0.0050$	0.805	7.7	3.1 <sup>a</sup>	$-0.926 \pm 0.062$	$1.025 \pm 0.035$
	820	3	$0.0913 \pm 0.0036$	0.805	7.7	1.0	$-0.955 \pm 0.038$	
	820 (sum)						$-0.947 \pm 0.032$	
	990	3	$0.0784 \pm 0.0060$	0.819	5.3	2.6 <sup>a</sup>	$-0.943 \pm 0.073$	$0.999 \pm 0.053$
	990	1	$0.0884 \pm 0.0066$	0.819	5.3	2.1 <sup>a</sup>	$-0.919 \pm 0.069$	
	990 (sum)						$-0.931 \pm 0.050$	
$Au^{198}, \beta^-$	460	1	$0.0755 \pm 0.0059$	0.869	4.4	8.2 <sup>a</sup>	$-0.789 \pm 0.062$	$0.935 \pm 0.051$
	460	1	$0.0748 \pm 0.0060$	0.869	4.4	10.2	$-0.800 \pm 0.065$	
	460 (sum)						$-0.795 \pm 0.045$	
	590	1	$0.0834 \pm 0.0045$	0.831	6.6	7.4	$-0.901 \pm 0.049$	
	810	1	$0.0846 \pm 0.0035$	0.805	7.7	4.8	$-0.919 \pm 0.038$	
$RaE, \beta^-$	520	1	$0.0610 \pm 0.0050$	0.861	4.4	3.7 <sup>a</sup>	$-0.613 \pm 0.050$	$0.715 \pm 0.060$
	640	1	$0.0615 \pm 0.0055$	0.816	6.6	2.6 <sup>a</sup>	$-0.645 \pm 0.058$	$0.726 \pm 0.065$
	810	2	$0.0655 \pm 0.0055$	0.805	7.7	2.4 <sup>a</sup>	$-0.777 \pm 0.066$	
	810	1	$0.0661 \pm 0.0041$	0.805	7.7	1.9 <sup>a</sup>	$-0.698 \pm 0.058$	
	810 (sum)						$-0.723 \pm 0.036$	$0.788 \pm 0.039$
	950	1	$0.0648 \pm 0.0050$	0.819	5.3	1.7 <sup>a</sup>	$-0.672 \pm 0.052$	$0.723 \pm 0.056$
$Ga^{68}, \beta^+$	1030	1	$0.0649 \pm 0.0103$	0.652	5.1	b	$0.830 \pm 0.131$	$-0.88 \pm 0.14$
	1300	1	$0.0880 \pm 0.0092$	0.695	4.5	b	$1.05 \pm 0.11$	$-1.10 \pm 0.12$

<sup>a</sup> Includes correction for scattering from source holder.

<sup>b</sup> Not calculated.

ator. The number of these electrons was measured with an absorber over the source that stopped direct electrons but allowed the scattered ones through. Their polarization was measured, and they were found to be depolarized by the amount expected after  $90^\circ$  scattering. The largest depolarization corrections were required for the  $Au^{198}$  source but these were the ones whose thickness was most uniform and most accurately known. No depolarization corrections were calculated for the  $Ga^{68}$  measurements because of their large statistical uncertainty. The corrections are roughly estimated at 1 to 2%.

For all measurements,  $\langle \cos \alpha \rangle_{av} = 0.860$ . For foil 1,  $f = 0.0698$ ; for foil 2,  $f = 0.0623$ ; and for foil 3,  $f = 0.0606$ . The uncertainty in the magnetic measurements on the foils was about  $\pm 2\%$ . If it is assumed that the gyromagnetic ratio  $g'$  for Supermendur (49% Fe, 49% Co, 2% Va) is somewhere between the values for  $Fe^{19}$  and  $Co$ ,<sup>20</sup> one has  $g' = 1.89 \pm 0.04$ . This assumption gives an uncertainty of about  $\pm 2\%$  in the value of  $f$ . If these uncertainties add randomly, the total uncertainty in  $f$  is about  $\pm 3\%$ .

In averaging  $R = (1 - \sigma_p/\sigma_a)/(1 + \sigma_p/\sigma_a)$  over scattering angles to obtain  $R_{av}$ , the quantity calculated was the relative decrease in  $R$  from its value for  $90^\circ$  scattering,  $[R(90^\circ) - R_{av}]/R(90^\circ)$ . Estimates of this correction by different methods were consistent within about  $\pm 20\%$ . However, in finding the widths of the accepted distributions of scattering angles, the large energy width passed by the monochromator and the energy resolution of the scintillation counter had to be subtracted from

the measured distributions. In some cases, the resulting distribution was not much wider than the distributions that were subtracted. It is probably safer to assume an uncertainty of about  $\pm 40\%$  in these corrections. Since they are generally about 5%, this adds another  $\pm 2\%$  uncertainty to the polarization.

The expressions used for  $\sigma_p/\sigma_a$  were calculated in lowest order. It is unlikely that this approximation leads to an error significant in comparison with other uncertainties in the experiment. Radiative corrections should be of order  $1/137$ ,<sup>17,28</sup> and  $\sigma_p/\sigma_a$  appears in the expression for the polarization in such a way that about a 5% error in  $\sigma_p/\sigma_a$  is necessary to cause a 1% error in the polarization.

Another possible source of error is the neglect of the binding of the target electrons to the nucleus, which could change the scattering cross section, or disturb the angular correlation of the two outgoing electrons and reduce the probability of counting them. Since the effect would be strongest for the unpolarized inner electrons, the effective value of  $f$  would be changed. At the energies used in this experiment (more than 70 times the  $K$  shell binding energy of iron) it is not likely that this effect is significant.

## 6. DISCUSSION OF RESULTS

### 6.1 $P^{32}$

$P^{32}$  has an allowed, Gamow-Teller, decay. Our results are consistent with  $(v/c)$  polarization, which is predicted

<sup>28</sup> A. Akhiezer and R. Polovin, Doklady Akad. Nauk S.S.S.R. **90**, 55 (1953).

for allowed decays by beta-decay theory, and in agreement with other measurements.

A slight deviation from ( $v/c$ ) polarization in this decay would not be inconsistent with current theory. Its  $ft$  value is large for an allowed decay ( $\log ft=7.9$ ) and the spectrum deviates slightly from allowed shape.<sup>29,30</sup> This large  $ft$  value has been explained by assuming that the decay is  $L$ -forbidden and second-order matrix elements make an appreciable contribution.<sup>31</sup> Such contributions might cause a deviation from  $v/c$  polarization. Bühring<sup>32</sup> has estimated the size of this possible deviation and concludes that it should decrease with increasing energy and be no greater than  $(-1.9^{+1.1})\%$  at  $v/c=0.7$ . Geshkenbein, however, has calculated the expected  $P^{32}$  polarization and finds<sup>33</sup>

$$P/(-v/c)=1-a/E,$$

where  $E$  is the total decay energy in units of  $mc^2$ . By fitting the spectrum shape, he predicts  $a=0.18$ . Such a deviation from a pure ( $v/c$ ) dependence is inconsistent with our results.

### 6.2 Au<sup>198</sup>

This is a first forbidden ( $2^- \rightarrow 2^+$ ) decay with an allowed spectrum shape. For such decays in high- $Z$  nuclei, the so-called  $\xi$ -approximation holds and ( $v/c$ ) polarization is expected.<sup>34</sup> Our results are consistent with ( $v/c$ ) polarization, and in agreement with other measurements.

### 6.3 Ga<sup>68</sup>

Ga<sup>68</sup> is an allowed, Gamow-Teller positron emitter. Our results show ( $v/c$ ) polarization, in agreement with current beta-decay theory. The relatively large statistical error quoted for these measurements is due only to the weakness of this source, and not to the fact that positrons were being measured.

### 6.4 RaE

RaE has always been of great interest for all investigations of beta decay. Again, in experiments on electron polarization, it turned out that RaE plays a special role; its polarization is considerably smaller than  $v/c$ . Our own results agree with other measurements<sup>11-14</sup> and hence help bearing out the theoretical predictions.<sup>35-37</sup>

According to the present theoretical interpretation of this decay, the cancellation of usually dominant matrix elements allows the effects of several smaller ones to be seen in the spectrum shape and electron polarization. Curtis and Lewis<sup>37</sup> pointed out that, in this case, a violation of time reversal invariance in the beta interaction should influence the electron polarization. Alikhanov's group<sup>18</sup> and Wegener<sup>14</sup> have since used measurements of RaE electron polarization in an attempt to test time reversal invariance.

The RaE spectrum shape and electron polarization can be expressed as functions of nuclear parameters and the parameters describing the beta decay interaction. The nuclear parameters are nuclear matrix elements and moments of the nuclear charge distribution entering in nuclear-size-effect calculations. In testing time-reversal invariance, one parameter of the beta-decay interaction—a possible imaginary part of the Fermi or Gamow-Teller interaction constant—is left adjustable. An exact knowledge of the spectrum shape and electron polarization should fix all the nuclear parameters and the imaginary part of one beta interaction constant. However, uncertainties in the measurements and in the very complicated calculations make it impossible to fix all the free parameters simultaneously. Therefore, a simplified analysis of the RaE problem is used, with a restricted number of nuclear parameters. With an analysis of this kind, Alikhanov's group fixes the phase angle between the Fermi and Gamow-Teller interaction constants as  $177.5^\circ_{-0.5}^{+2.5}$ . Wegener finds a deviation from  $0^\circ$  or  $180^\circ$  of  $1.6 \pm 8^\circ$ . If our data were included in these analyses, their conclusions would not be changed in any important way.

Both of these analyses use only two adjustable nuclear parameters. According to Newby and Konopinski,<sup>38</sup> at least one more should be used in an analysis of the RaE decay. Other published analyses<sup>34,39</sup> use five, or even eight. The conclusions concerning time-reversal invariance are hence open to some doubt.

The RaE electron polarization data can be put to another interesting use. If the Fermi—Gamow-Teller phase angle is assumed to be  $180^\circ$  from the measurements on polarized neutrons, it should be possible to fix all the nuclear parameters without resorting to a simplified analysis. There are now at least three accurate sets of measurements of the RaE electron polarization, covering the energy region between 128 and 950 keV, using a variety of techniques, and consistent with each other where measurements were made near the same energy. With all these data to fit, even a large number of nuclear parameters should be fixed with reasonable accuracy. The values of these parameters may be of great interest. As Newby and Konopinski<sup>38</sup> have pointed out, their values as calculated from a

<sup>29</sup> O. E. Johnson, R. G. Johnson, and L. M. Langer, Phys. Rev. **112**, 2004 (1958).

<sup>30</sup> F. T. Porter, F. Wagner, Jr., and M. S. Freedman, Phys. Rev. **107**, 135 (1957).

<sup>31</sup> I. Iben, Phys. Rev. **109**, 2059 (1958).

<sup>32</sup> W. Bühring, Z. Physik **155**, 566 (1959).

<sup>33</sup> B. B. Geshkenbein, J. Exptl. Theoret. Phys. (U.S.S.R.) **38**, 1341 (1960) [translation: Soviet Phys. JETP **11**, 965 (1960)].

<sup>34</sup> T. Kotani and M. Ross, Progr. Theoret. Phys. (Kyoto) **20**, 643 (1958).

<sup>35</sup> J. Fujita, M. Yamada, V. Matumoto, and S. Nakamura, Phys. Rev. **108**, 1104 (1957).

<sup>36</sup> A. Bincer, E. Church, and J. Weneser, Phys. Rev. Letters **1**, 95 (1958).

<sup>37</sup> R. B. Curtis and R. R. Lewis, Phys. Rev. **107**, 543 (1957).

<sup>38</sup> N. Newby and E. J. Konopinski, Phys. Rev. **115**, 1434 (1959).

<sup>39</sup> Z. Matumoto and M. Yamada, Progr. Theoret. Phys. (Kyoto) **19**, 285 (1958).

nuclear model are strongly affected by the conserved vector current theory of beta decay. It remains questionable, however, whether a meaningful comparison of theoretical and experimental parameters will be possible. The accuracy of the nuclear model calculations is doubtful at best, and the calculation of the conserved vector current effects will not be easy. However, in view of the present lack of a clear experimental test of the theory, this approach may be worth more investigation.

**APPENDIX. AVERAGING  $R = (1 - \sigma_p/\sigma_a)/(1 + \sigma_p/\sigma_a)$  OVER THE ACCEPTED COINCIDENCES**

In the following equations,  $\gamma$  is the initial total energy of the incident electron in the laboratory system in units of  $mc^2$ ;  $\beta = v/c$  for either electron in the c.m. system; and  $x = 1 - 2W$ , where  $W$  is the fraction of the incident electron's kinetic energy which is transferred to the other electron in the collision. The parameter  $x$  is equal to  $\cos\theta'$ , where  $\theta'$  is the c.m. scattering angle, so  $x=0$  for a collision with a  $90^\circ$  scattering angle.

The average value of  $R$  over the accepted coincidences is

$$R_{av} = \int_{-1}^1 R(x)N(x)dx, \quad (13)$$

where  $N(x) = dN/dx$  is the normalized distribution of counted events per unit energy partition parameter  $x$ . The accepted distribution of electrons is centered on a  $90^\circ$  scattering angle in the c.m. system so  $N(x)$  will be centered on  $x=0$ . If  $N(x)$  is narrow enough, it should be possible to represent  $R(x)$  accurately in the region where  $N(x)$  is large with a few terms of a power series expansion about  $x=0$ :

$$R(x) = R(0)[1 + A_1x + A_2x^2 + \dots]. \quad (14)$$

This expansion gives

$$\begin{aligned} R_{av} &= R(0) \left[ 1 + A_1 \int_{-1}^1 xN(x)dx + A_2 \int_{-1}^1 x^2N(x)dx + \dots \right] \\ &= R(0)[1 + A_1x_{av} + A_2(x^2)_{av} + \dots]. \end{aligned} \quad (15)$$

It is then possible to express  $R_{av}$  in terms of a few moments of  $N(x)$ . If  $N(x)$  can be represented by some well-known function, these moments may be easy to calculate.

Power series expansions of  $R$  can be calculated from the expressions for  $\sigma_p$ ,  $\sigma_a$ , and  $\sigma_p/\sigma_a$  given by Bincer.<sup>15</sup> For electron-electron collisions,  $R$  can be written down from Bincer's expression for  $\sigma_p/\sigma_a$  and expanded. For electron-positron collisions, since our apparatus does

not distinguish between electrons and positrons,  $\sigma_p$  must be replaced by  $\sigma_p(x) + \sigma_p(-x)$ , and likewise for  $\sigma_a$ . This procedure gives the cross section for a collision resulting in an electron or a positron of energy parameter  $x$ .  $R$  is then formed from these sums of cross sections and expanded. For both kinds of collisions, (15) can be written as

$$\begin{aligned} R_{av} &= \frac{C_0}{K_0} \left[ 1 + \left\{ \frac{C_1}{C_0} - \frac{K_1}{K_0} \right\} (x^2)_{av} \right. \\ &\quad \left. + \left\{ \frac{K_1^2}{K_0^2} - \frac{C_1K_1}{C_0K_0} + \frac{C_2}{C_0} - \frac{K_2}{K_0} \right\} (x^4)_{av} + \dots \right]. \end{aligned} \quad (16)$$

For electron-electron collisions:

$$\begin{aligned} C_0 &= 7\gamma^2 - 6\gamma + 3, \\ C_1 &= -6\gamma^2 + 8\gamma - 6, \\ C_2 &= -\gamma^2 - 2\gamma + 3, \\ K_0 &= 9\gamma^2 - 10\gamma + 5, \\ K_1 &= 6\gamma^2 + 12\gamma - 6, \\ K_2 &= \gamma^2 - 2\gamma + 1. \end{aligned}$$

For electron-positron collisions, with electrons and positrons not distinguished:

$$\begin{aligned} C_0 &= 4\beta^2 + 3\beta^4, \\ C_1 &= 6\beta^2 + 8\beta^4 + \beta^8, \\ C_2 &= 6\beta^2 + 8\beta^4 + 2\beta^6, \\ K_0 &= 4 - 6\beta^2 + 13\beta^4 - 2\beta^6, \\ K_1 &= 12 + 10\beta^2 + 8\beta^4 + 2\beta^6 + \beta^8, \\ K_2 &= 20 + 26\beta^2 + 16\beta^4 + 2\beta^6. \end{aligned}$$

Our measured distributions of events were fitted very well by Gaussians. At the energies used in this experiment, the coefficients of  $(x^2)_{av}$  and  $(x^4)_{av}$  were of about the same size and the  $1/e$  widths of the distributions were generally about 0.25. It was only necessary to use the second-order term.

**ACKNOWLEDGMENTS**

We wish to thank Dr. A. O. Hanson and Dr. N. Levine for help and many invaluable suggestions during the early phases of the present work. We are deeply grateful to G. DePasquali for the preparation of the radioactive sources and to J. Lemak for his assistance during the measurements. We are indebted to Dr. H. L. B. Gould for providing us with the ferromagnetic foils and to Dr. E. J. Konopinski and Dr. J. Weneser for valuable discussions.